



Aerosol modeling over Europe: 2. Interannual variability of aerosol shortwave direct radiative forcing

E. Marmor,^{1,2} B. Langmann,^{1,3} K. Hungershofer,^{4,5} and T. Trautmann^{4,6}

Received 15 September 2006; revised 25 May 2007; accepted 13 June 2007; published 3 October 2007.

[1] Aerosol distribution over Europe and its direct radiative forcing have been simulated with a regional atmosphere-chemistry model and an off-line radiation transfer model. Primary and secondary organic and inorganic aerosols have been considered. The simulation was conducted for meteorologically different years 2002 and 2003 to analyze the spatial and temporal variability of the aerosol distribution and the direct forcing. The accompanying paper focuses on the aerosol distribution, while radiative forcing is discussed in this paper. The mixing state of aerosols, externally or internally, is shown to influence the strength, regional distribution and sign of radiative forcing, thereby regulating the forcing efficiency. Positive top-of-the-atmosphere forcing was simulated over eastern and southeastern Europe in spring and winter because of contribution of black carbon. Its strength varies from +0.2 to +1 W m⁻², depending on aerosol mixing assumptions. Sensitivity studies show a mean European direct forcing of -0.3 W m⁻² in winter and -2.5 W m⁻² in summer, regionally ranging from -5 to +4 W m⁻².

Citation: Marmor, E., B. Langmann, K. Hungershofer, and T. Trautmann (2007), Aerosol modeling over Europe: 2. Interannual variability of aerosol shortwave direct radiative forcing, *J. Geophys. Res.*, 112, D23S16, doi:10.1029/2006JD008040.

1. Introduction

[2] Determining the aerosol impact on climate presents a great challenge for the climate research. The direct aerosol forcing results from the ability of aerosol particles to scatter and/or absorb solar radiation. Direct aerosol forcing estimates require a detailed knowledge of the regional aerosol distribution, its chemical composition and the mixing state. The sensitivity of the modeled European climate to a change in its aerosol direct forcing due to different aerosol distributions was investigated by *Hohenegger and Vidale* [2005], emphasizing the importance of the accuracy of the predicted aerosol distribution.

[3] Relatively few studies have investigated the direct radiative forcing resulting from organic aerosol [*Kanakidou et al.*, 2005, and references therein]. A considerable fraction of total organic aerosol is thought to be secondary (30 to 80% [*Gelencsér et al.*, 2007]), therefore its contribution to aerosol pollution and forcing should be considered. Only in the work

by *Chung and Seinfeld* [2002] has secondary organic aerosol formation been treated explicitly.

[4] The radiative forcing of externally mixed aerosol is determined by adding up the forcings exerted by individual aerosol compounds. This assumption is acceptable for newly released aerosols, but aged particles are found to be mixed internally [e.g., *Murphy and Thomson*, 1997; *Middlebrook et al.*, 1998]. Observations of the aerosol mixing state over Europe are sparse. For the urban aerosol in southern France, black carbon was observed to be mixed externally with other species [*Mallet et al.*, 2004]. Other studies had shown that the Vienna aerosol (urban) is partially internally mixed with respect to both black carbon [*Hitzenberger and Tohno*, 2001] and total carbon [*Hitzenberger and Puxbaum*, 1993], while aerosols sampled at the remote site of Sonnblick (over 3000 m asl) where found to be partially externally mixed [*Kasper-Giebl et al.*, 2000]. Considering the internal mixing of sulfate and black carbon aerosols can substantially alter forcing estimates [e.g., *Myhre et al.*, 1998; *Lesins et al.*, 2002]. *Lesins et al.* [2002] showed that for specific internal mixing assumptions nearly all of the cooling effect predicted for the external mixture is set off by the black carbon absorption enhancement.

[5] Regional and temporal distribution of this forcing also depends on meteorological conditions. Partially absorbing aerosol may exert a local negative forcing over regions with low surface albedo and a positive forcing over regions with high surface albedo [e.g., *Chylek and Wong*, 1995]. Similar results are found if partially absorbing aerosol resides above clouds with high albedo [*Haywood et al.*, 1997].

[6] All forcing estimates described above utilized global climate models, whose coarse resolution leads to the

¹Max Planck Institute for Meteorology, Hamburg, Germany.

²Now at Joint Research Centre, Ispra, Italy.

³Now at Department of Experimental Physics, National University of Ireland, Galway, Ireland.

⁴Institute for Meteorology, University of Leipzig, Leipzig, Germany.

⁵Now at Laboratoire Interuniversitaire des Systèmes Atmosphériques, Centre National de la Recherche Scientifique/Université Paris 7 and 12, Créteil, France.

⁶Also at Remote Sensing Technology Institute, German Aerospace Centre, Wessling, Germany.

Table 1. Aerosol Physical and Optical Properties as Found in Literature

Author	Aerosol	r_{eN_s} , μm	σ_g	Density, $\text{kg}(\text{m}^{-3})$	Refractive Indices at 0.55 μm
Langmann et al. [1998]	sulfate	0.05	1.8	1600	1.43 -i 2.0*10 ⁻⁸
Hess et al. [1998]	sulfate	0.1	2.0	1760	1.53 -i 6.0*10 ⁻³
Koepke et al. [1994]	sulfate	0.07	2.03	1700	1.43 -i 1.0*10 ⁻⁸
Penner et al. [1998]	sulfate	0.05	2.0	1200	1.53 -i 1.0*10 ⁻⁷
Penner et al. [1998]	BC	0.0118	2.0	1800	1.75 -i 4.4*10 ⁻¹
Hess et al. [1998]	BC	0.01	2.0	1000	1.75 -i 4.4*10 ⁻¹
Cooke et al. [1999]	OC	0.02	2.0	1800	
This study	sulfate	0.05	1.8	1600	1.53 -i 1.0*10 ⁻⁷
This study	BC	0.0118	2.0	1800	1.75 -i 4.4*10 ⁻¹
This study	OC	0.05	2.0	1200	1.53 -i 1.0*10 ⁻⁷

smoothing of local inhomogeneities of the aerosol distribution. To improve on this, we have utilized a regional atmosphere-chemistry model over Europe to simulate aerosol mass distribution for the years 2002 and 2003 [see Marmer and Langmann, 2007]. Sulfate, black carbon and primary and secondary organic carbon aerosols have been included. We have also utilized an off-line radiation transfer model to determine the direct aerosol forcing assuming both externally and internally mixed aerosols. The dependency of this forcing on aerosol burden distribution and meteorological conditions is further analyzed. Finally, we have performed a sensitivity experiment determining the direct forcing of the aerosol burden scaled to measurements. The experiment result is considered to be a more realistic estimate of the European aerosol forcing.

2. Experimental Setup

2.1. Regional Atmosphere Chemistry Model REMOTE

[7] The regional atmosphere chemistry model REMOTE (Regional Model with Tracer Extension) [Langmann, 2000] was initially applied to determine the aerosol distribution over Europe.

[8] REMOTE determines the physical and chemical state of the modeled atmosphere at every time step. The horizontal resolution for this study is 0.5 °, the modeled atmosphere contains 19 hybrid pressure levels extending up to 10 hPa. On the lateral boundaries, the model was driven with ECMWF meteorological analysis data every 6 hours. The dynamical part of the model is based on the global ECHAM 4 model [Roeckner, 1996; Jacob, 2001]. The stratiform cloud scheme is based on the approach from Sundquist [1978]. Subgrid cloud formation is included by incorporating fractional cloud cover (parameterized as a nonlinear function of grid mean relative humidity) for each grid box. The convective cloud module is based on the scheme of Tiedtke [1989] and is formulated as bulk mass flux scheme, determining the overall mass flux of all cumulus clouds in one grid column. The simulated cloud coverage has been evaluated by M. Reuter and J. Fischer (A comparison of measured and simulated cloud coverage in the Baltic Sea area as part of the BALTIMOS project, submitted to Theoretical and Applied Climatology, 2007), the water vapor has been compared with measurements by R. Leinweber and J. Fischer (Water vapour in BALTIMOS: A comparison with MODIS measurements, submitted to Theoretical and Applied Climatology, 2007). The back-

ground surface albedo over snow-free land areas is prescribed by the land surface data set of Hagemann [2002]. Over snow and sea ice, the albedo is modified by surface conditions during the model simulation. The sea ice albedo is diagnosed from surface temperature regardless of any surface characteristics. The snow albedo depends on the vegetation cover and is calculated from the diagnosed snow depth and surface temperature. The snow and sea ice albedo parameterization has been evaluated by Roesch et al. [2001], Koltzow and Eastwood [2002], and Koltzow et al. [2003].

[9] Considered aerosols, sulfate, black and organic carbon, are treated as a bulk mass. Chemical initial and boundary conditions were prescribed by the model results of the global chemistry transport model MOZART [Horowitz et al., 2003] for species that are common to both REMOTE and MOZART. Concentrations of the other species are derived from available measurements [Chang et al., 1987, and references therein] and are held constant at lateral model boundaries throughout the simulation. Emissions of SO_x , NO_x , NH_3 , CO and VOC for the year 2001 and of $\text{PM}_{2.5}$ for the year 2000 with monthly emission factors for each country and emission sector have been applied for the simulations of both years, 2002 and 2003 [Vestreng et al., 2004]. Chemical speciation of $\text{PM}_{2.5}$ emissions into primary organic carbon (POC) and black carbon (BC) is based on Andersson-Skold and Simpson [2001]. Primary biogenic emissions of organic carbon [Puxbaum and Tenze-Kunit, 2003] and emissions from forest fires [Hodzic et al., 2007] have not been considered. Biogenic VOC emissions are calculated in REMOTE as a function of temperature, solar radiation and land use, based on the approach of Guenther et al. [1991, 1993]. Secondary organic aerosol production is calculated according to the approach of Schell [2000]. The results of this simulations are discussed in this issue [Marmer and Langmann, 2007].

2.2. Radiation Transfer Model ORTM

[10] The direct radiative shortwave aerosol forcing was then calculated using the Off-line Radiation Transfer Model (ORTM) described by Langmann et al. [1998] on the basis of the variable aerosol mass distribution and meteorological input data modeled by REMOTE (section 2.1). The delta-Eddington approximation includes single as well as multiple scattering. Only the shortwave part of the solar spectrum 0.2–5 μm , subdivided into 18 wavelength intervals, is considered, because aerosols considered here have a negligible radiative effect in the infrared. Optical properties of

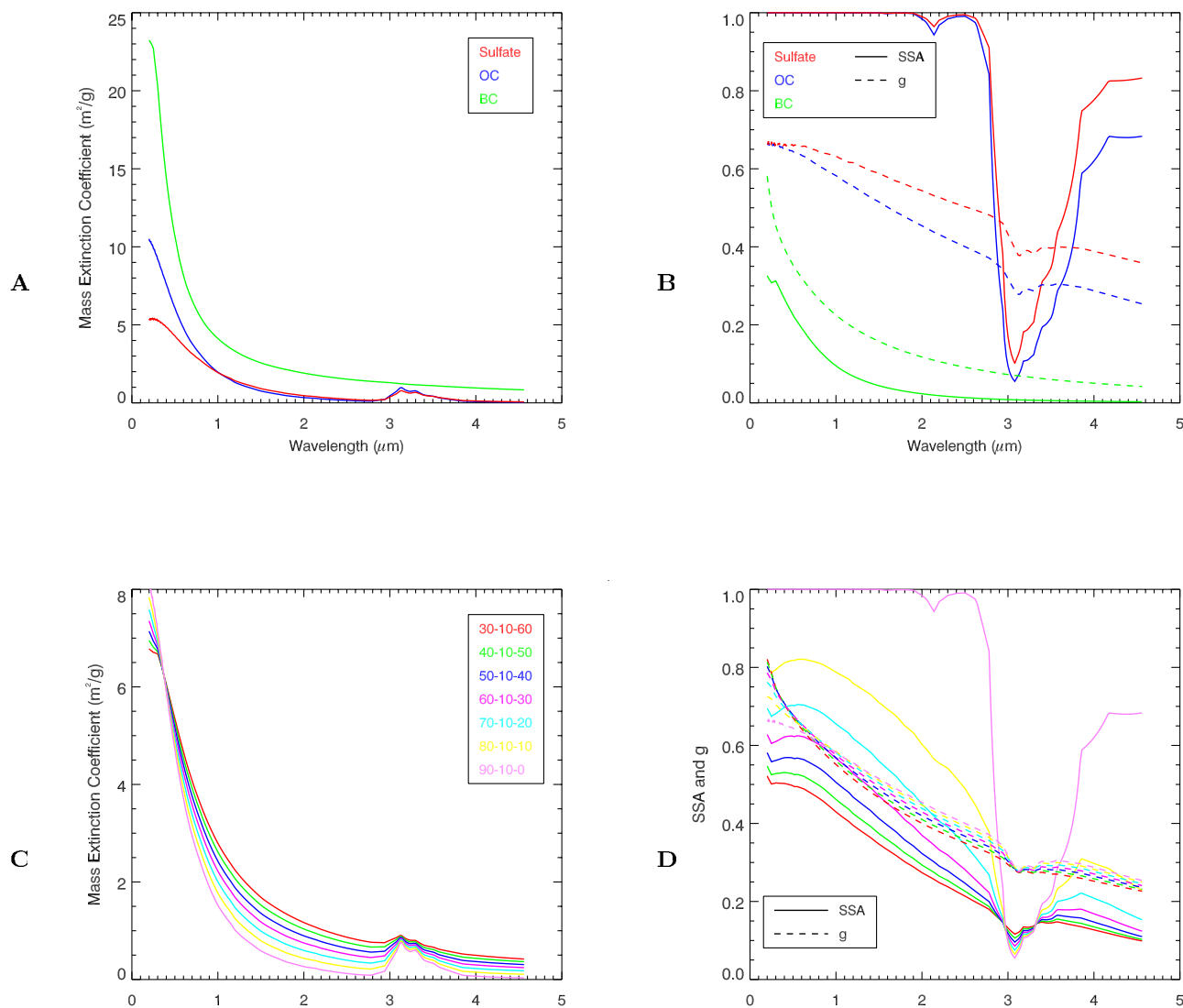


Figure 1. (a) Mass extinction coefficient and (b) single scattering albedo (SSA) and asymmetry factor g as a function of the wavelength for externally mixed aerosols. (c) Mass extinction coefficient and (d) single scattering albedo (SSA) and asymmetry factor g as a function of the wavelength for internally mixed aerosols. Examples for eight different internal mixtures with mass contributions of sulfate-OC-BC (%) for the internally mixed aerosols are shown in Figures 1c and 1d. The scales of the mass extinction coefficient are different for externally (Figure 1a) and internally (Figure 1c) mixed aerosols.

the dry sulfate aerosol are determined from Mie theory calculations. The modification of aerosol specific extinction due to relative humidity of the ambient air is considered using a simple approximation adapted from the data given by *Nemesure et al.* [1995]. For relative humidities (RH) below 80%, the specific extinction is enhanced by a factor of $\text{RH} \times 0.04$, assuming a minimum RH of 25%. For RH exceeding 80%, the specific extinction increases exponentially with RH. The factor 9.9 is reached for $\text{RH} = 100\%$. Exponential growth is assumed for hygroscopic aerosols (sulfate and organic carbon in case of external mixing as well as for internally mixed aerosols). Black carbon, if externally mixed, is assumed to be mostly hydrophobic and its specific extinction increases only linearly with RH. Single scattering albedo and the asymmetry factor are

assumed to be independent of RH. This approach might result in a small overestimation of the shortwave radiative forcing of scattering aerosols, because with increasing relative humidity forward scattering is increased and back-scattering in space direction reduced (asymmetry factor increased).

[11] In this study, the forcing due to natural and anthropogenic aerosols have not been distinguished. While some natural sources of sulfur such as DMS and volcanoes have been included, only anthropogenic sources of primary carbonaceous aerosols could be considered. The emission inventory applied does not include biomass burning emissions from forest fires [*Marmer and Langmann, 2007*]. Secondary organic aerosol (SOA) formed from oxidized volatile organic compounds (VOCs) emitted by vegetation

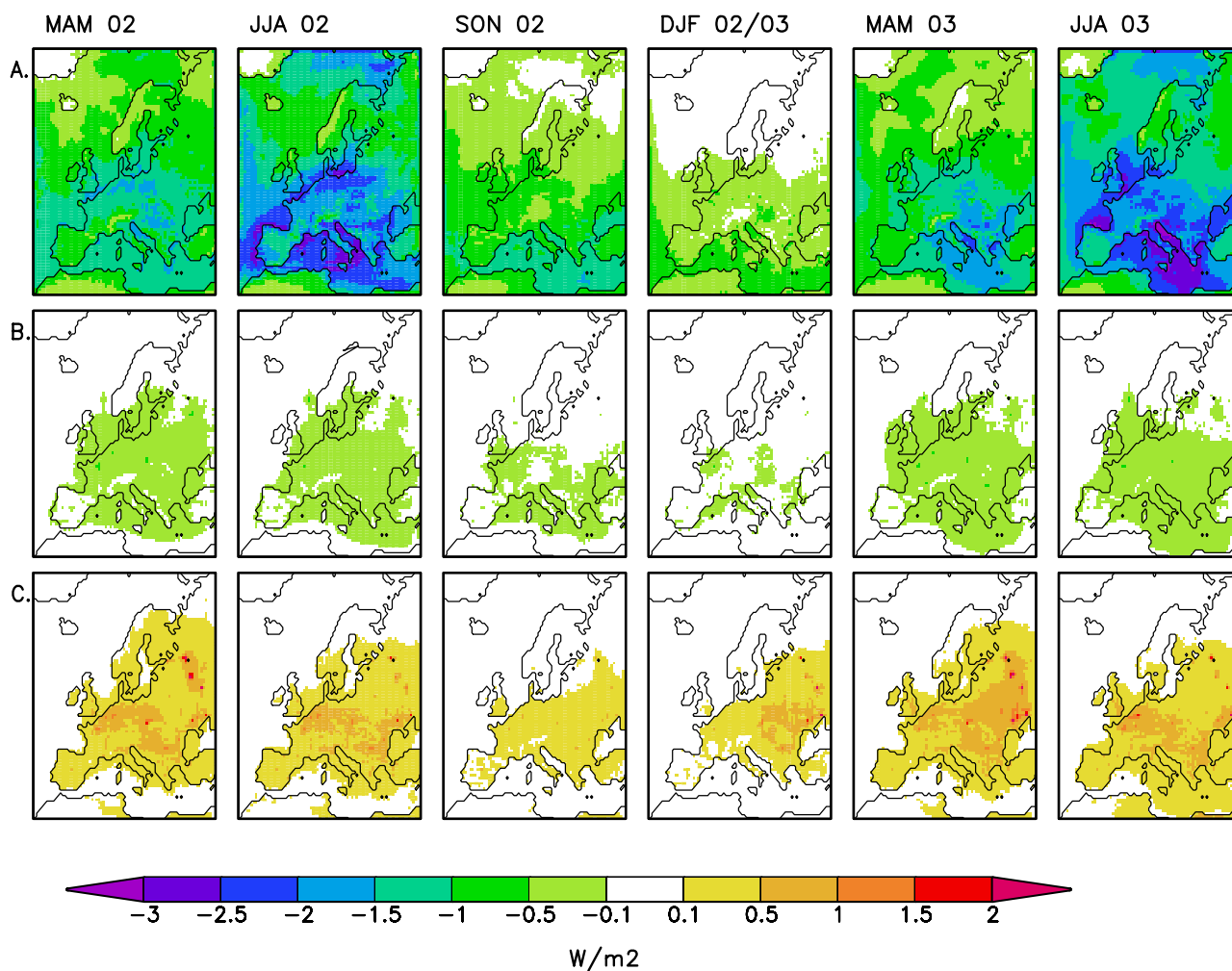


Figure 2. Seasonal mean direct radiative forcing of (a) sulfate aerosol, (b) organic carbon and (c) black carbon (W m^{-2}) for March–April–May (MAM), June–July–August (JJA), September–October–November (SON) and December–January–February (DJF), 2002–2003.

has been considered, but its formation involves photo-oxidants, whose concentration levels directly depend on human activity. Thus biogenic SOA cannot be considered purely natural [Kanakidou *et al.*, 2000].

2.3. Aerosol Optical Properties

[12] The ORTM has been extended for this work to include (organic carbon) OC and BC (black carbon) aerosol in addition to sulfate. The broadband aerosol optical properties were determined in two steps: First, the spectral optical properties in the wavelength region between $0.2 \mu\text{m}$ and $5 \mu\text{m}$ were calculated on the basis of Mie theory. In a second step, these spectral quantities were weighted by the extraterrestrial solar flux [Wehrli, 1985], and averaged over the applied wavelength intervals of the ORTM. REMOTE determines aerosol mass, and does not provide information about particle size distributions or particle densities, so we had to make assumptions about these properties for the Mie calculations. In Table 1, assumptions made by different authors, demonstrating substantial differences, are presented. In this study, a lognormal size distribution with a geometric mean radius of $0.05 \mu\text{m}$ for sulfate and OC

[Penner *et al.*, 1998], a geometric standard deviation σ_g of 1.8 for sulfate and 2.0 for OC, and a particle density of $1600 \text{ kg}(\text{m}^{-3})$ [Langmann *et al.*, 1998] and $1200 \text{ kg}(\text{m}^{-3})$ [Turpin and Lim, 2001], respectively have been assumed. Wavelength-dependent complex refractive indices for sulfate were taken from Toon *et al.* [1976]. The same values were assumed for organic carbon [Sloane, 1983]. The geometric mean radius for BC particles is assumed to be $0.0118 \mu\text{m}$ with a sigma of 2.0 and a particle density of $1800 \text{ kg}(\text{m}^{-3})$ [Penner *et al.*, 1998]. For the refractive indices, the values from Fenn *et al.* [1985] were applied.

[13] In case of an internal mixture of sulfate, black and organic carbon a monomodal lognormal size distribution with a geometric mean radius of $0.05 \mu\text{m}$ and a geometric standard deviation σ_g of 2.0 was assumed. The chemical composition of the internally mixed aerosol for every grid box was determined from the volume of sulfate, BC and OC in 10% intervals. An effective refractive index for the mixture was retrieved from the refractive indices of the single components with the volume-weighted mixture approach. Similarly, a mean particle density was determined.

Table 2. Calculated Seasonal Mean and Maximum Values of the Direct Radiative Forcing of Each Aerosol Type for March–April–May (MAM), June–July–August (JJA), September–October–November (SON), and December–January–February (DJF), 2002–2003^a

	Sulfate	BC	OC
MAM 2002			
Mean	−0.8	+0.16	−0.08
Maximum	−2.4	+4.4	−0.91
JJA 2002			
Mean	−1.4	+0.15	−0.07
Maximum	−3.9	+1.8	−0.9
SON 2002			
Mean	−0.5	+0.06	−0.05
Maximum	−1.7	+0.9	−0.5
DJF 2002/2003			
Mean	−0.2	+0.08	−0.03
Maximum	−1.2	+2.2	−0.6
MAM 2003			
Mean	−0.8	+0.18	−0.09
Maximum	−2.4	+3.8	−0.8
JJA 2003			
Mean	−1.5	+0.15	−0.08
Maximum	−4.1	+2.0	−0.9

^aUnit is W m^{-2} .

Optical properties as a function of wavelength for external and internal mixture are presented in Figure 1.

3. Model Results

[14] The radiation flux density at the top of the atmosphere (TOA) was calculated with and without aerosols. The forcing is restricted to solar spectral range. The direct radiative forcing was calculated for individual aerosol compounds, and for externally and internally mixed aerosols.

3.1. Externally Mixed Aerosols

3.1.1. Sulfate

[15] Sulfate aerosol particles scatter shortwave radiation, so that a part of the incoming solar radiation is scattered back to space, resulting in a negative forcing at the top of the atmosphere [Haywood and Boucher, 2000]. Direct radiative shortwave forcing of sulfate aerosol shows annual and interannual variabilities (Figure 2a).

[16] The seasonal mean of the direct forcing of sulfate aerosol over Europe varies from -0.2 W m^{-2} in winter to -1.5 W m^{-2} in summer (Table 2). The forcing pattern is different for the same seasons of the different years: the mean values slightly vary with stronger forcing in spring and summer 2003, compared to 2002. In summer 2003, the maximum of -4.3 W m^{-2} over the Mediterranean is significantly higher than in the previous year.

3.1.2. Carbonaceous Aerosols

[17] Organic carbon scatters shortwave radiation, just like sulfate, and has a negative TOA forcing. Seasonal means for summer and winter of the direct forcing due to organic carbon are presented in Figure 2b. The mean summer forcing of primary organic carbon is only -0.07 W m^{-2} in 2002 and -0.08 W m^{-2} in 2003; the mean winter forcing is -0.03 W m^{-2} (Table 2). These values are negligible compared with the direct forcing of sulfate aerosols. Sec-

ondary organic carbon contributes to the OC forcing mainly in summer, with maximum contribution of up to -0.3 W m^{-2} over Scandinavia in summer 2002 and over northern Italy in summer 2003 (not shown).

[18] Black carbon strongly absorbs shortwave radiation, thus its radiative TOA forcing is positive. Seasonal means for summer and winter of the direct forcing due to black carbon are presented in Figure 2c. The mean forcing of BC aerosol has a maximum during spring with $+0.16 \text{ W m}^{-2}$ in 2002 and $+0.18 \text{ W m}^{-2}$ in 2003 (Table 2), with forcing maxima of $+4.4 \text{ W m}^{-2}$ in 2002 and $+3.8 \text{ W m}^{-2}$ in 2003 over northwestern Russia. The mean forcing is weakest during fall with $+0.06 \text{ W m}^{-2}$.

[19] Concentration of both, black and organic carbon, is underestimated by the model [Marmer and Langmann, 2007], so the calculated forcing can only be regarded as a minimum estimate. In Figure 3a we show the total direct shortwave forcing over Europe for winter and summer, assuming externally mixed aerosols, by adding up the different aerosol forcings to obtain the total forcing. This assumption is only an approximation, since aerosols are mixed externally and internally, and the optical properties of internal mixtures are different and not necessarily additive.

[20] The patterns of the seasonal mean forcing in summer and fall look very similar to the forcing of sulfate aerosols. In fall, black and organic carbon nearly compensate each other, since their forcing is of the same magnitude, but opposite in sign. In summer, the positive BC forcing is twice as strong as the negative OC forcing, but still an order of magnitude weaker than the negative sulfate forcing. Only over some areas the negative forcing is slightly enhanced by organic carbon or reduced by black carbon. In winter and spring, the forcing of black carbon dominates over eastern Europe. Here the emissions of black carbon due to domestic heating are responsible for the positive direct forcing of $+0.1$ to $+0.5 \text{ W m}^{-2}$, and up to $+3 \text{ W m}^{-2}$ over strong emission sources, this effect being magnified by the enhanced surface albedo (section 4).

3.2. Internally Mixed Aerosol Particles

[21] Estimates of the total aerosol forcing depend on the assumed mixing state of the aerosols [Lesins *et al.*, 2002]. At one extreme each aerosol component can be assumed to be physically separated from the other component creating an external mixture of chemically pure modes (section 3.1). At the other extreme, the aerosols can be assumed to be internally mixed as a homogeneous material reflecting the chemical and physical average of all contributing components. The real mixing state can be expected to lie somewhere in between these two extremes and is related to aerosol age [e.g., Murphy and Thomson, 1997; Middlebrook *et al.*, 1998; Hitzenberger and Tohno, 2001]. Freshly emitted aerosol particles are usually externally mixed, while aged particles are generally internally mixed. Even if the particles are individually pure when emitted, there are numerous processes in the atmosphere that can cause internal mixing: coagulation, cycling of aerosols through a cloud, aqueous reactions, gas-to-particle reaction onto existing particles [Lesins *et al.*, 2002]. The optical properties of internally mixed particles depend on their chemical composition. We have determined the total aerosol direct forcing assuming an internal mixing for all particles. Since our

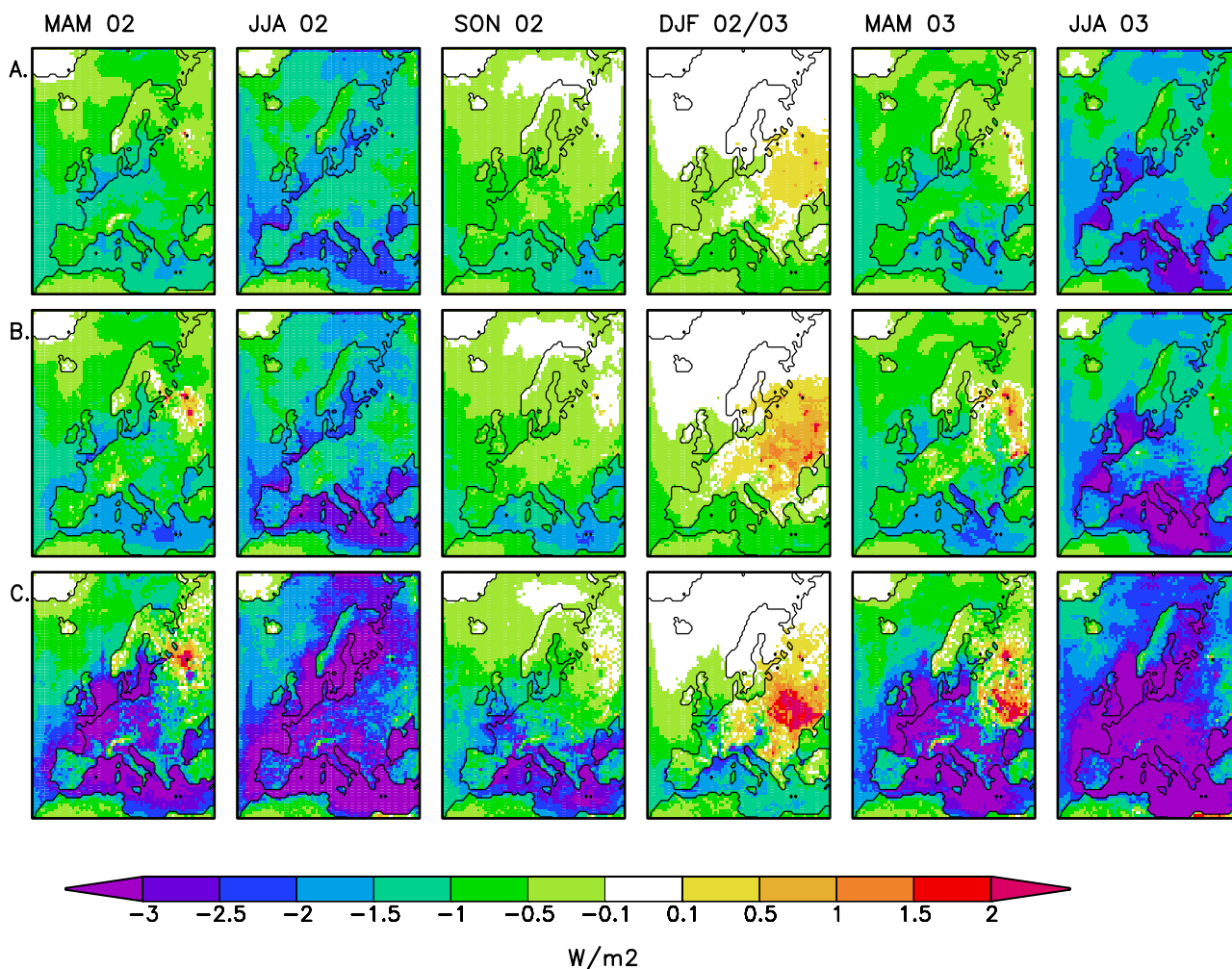


Figure 3. Seasonal mean direct radiative forcing of (a) externally mixed aerosols, (b) internally mixed aerosols and (c) internally mixed aerosols in a sensitivity experiment with BC burden multiplied by 2, OC burden multiplied by 10 (W m^{-2}) for March–April–May (MAM), June–July–August (JJA), September–October–November (SON) and December–January–February (DJF), 2002–2003.

aerosol simulation does not include internal mixing of aerosols (in REMOTE the aerosols are treated as bulk mass (sections 2.1 and 2.3)), the mixing state has no effect on the aerosol load. The internal mixing is considered here for radiation purposes only. Both positive and negative mean forcings (Figure 3b) exceed that of externally mixed aerosols.

[22] The most interesting feature is the enhancement of the positive forcing in spring and winter, which are the seasons with enhanced black carbon emissions. In spring, the forcing is positive over western Russia and the Alps, in winter over most of Europe. The reason for the higher absorption of internally mixed particles is that the absorption of a given amount of BC in a particle consisting of nonabsorbing material (sulfate, OC) is greater than that for the same amount of pure BC particles in air [Bohren, 1986]. Compared to the results of an external mixture (Figure 3a), the higher absorption of internally mixed aerosol including black carbon reduces the negative forcing (e.g., over France) and increases the positive forcing over western Russia in spring and over most of Europe in winter. In

regions where the contribution of black carbon is negligible, i.e., mainly over water and, e.g., the Iberian Peninsula, the negative forcing is increased. This increase of negative forcing is due to the assumed size distribution (section 2.3) which results in a larger backscattering in case of an internal mixture compared to an external mixture of sulfate and organic carbon.

[23] According to our estimates, our model captures only 50% of black and 10% of organic carbon concentrations partly because of the lack (forest fires) or underestimation (agricultural, waste and residential sources) of biomass burning emissions in our inventory [Simpson *et al.*, 2007]. To determine a maximum estimate of the direct forcing over Europe, we have run a sensitivity experiment, whereby we have doubled the atmospheric concentration of black carbon and multiplied that of the organic carbon by a factor of 10, assuming internally mixed aerosols (Figure 3c). The regional maxima in the sensitivity experiment are not realistic because biomass burning emissions distribution will differ from that of the anthropogenic sources. Comparing the minimum estimate, where we have assumed externally

Table 3. Seasonal Minimum, Mean, and Maximum Values of the Direct Radiative Forcing of the Total Aerosol Assuming External and Internal Mixing and for the Sensitivity Experiment for March–April–May (MAM), June–July–August (JJA), September–October–November (SON), and December–January–February (DJF), 2002–2003^a

	Externally Mixed	Internally Mixed	Internally Mixed, Sensitivity
MAM 2002			
Mean	−0.8	−0.9	−1.5
Minimum	−2.4	−2.3	−9.7
Maximum	+3.6	+7.2	+12.9
JJA 2002			
Mean	−1.4	−1.5	−2.4
Minimum	−3.4	−4.1	−10.4
Maximum	+0.1	+0.5	+0.6
SON 2002			
Mean	−0.5	−0.6	−1.0
Minimum	−1.9	−2.2	−5.1
Maximum	+0.4	+0.8	+4.6
DJF 2002/2003			
Mean	−0.2	−0.1	−0.3
Minimum	−1.2	−1.2	−5.3
Maximum	+2.1	+4.0	+4.6
MAM 2003			
Mean	−0.8	−0.8	−1.5
Minimum	−2.5	−2.7	−9.7
Maximum	+2.5	+4.9	+8.1
JJA 2003			
Mean	−1.5	−1.7	−2.7
Minimum	−4.3	−5.5	−11.5
Maximum	+0.5	+0.8	+1.7

^aUnit is $W\ m^{-2}$.

mixed aerosols (section 3.1), with this more realistic estimate, we find the mean direct forcing doubled in spring and fall, and increased by a factor of 1.5 in summer and winter (Table 3). The regional seasonal maxima of both positive and negative forcing show much greater enhancement: a factor 4 for the negative forcing in spring, and a factor 11 for the positive maximum in fall.

[24] Our forcing estimates have been compared to the results of other studies (Table 4). The annual mean direct forcing of externally mixed aerosols ($-0.74\ W\ m^{-2}$) compares well with the study of Koch *et al.* [2007] ($-0.83\ W\ m^{-2}$). A closer look reveals that this agreement is only due to averaging: Our sulfate forcing ($-0.76\ W\ m^{-2}$) is 1.4 times weaker than that of Koch *et al.* [2007] ($-1.13\ W\ m^{-2}$), just like the OC forcing ($-0.1\ W\ m^{-2}$ versus $-0.5\ W\ m^{-2}$), and our BC forcing is 4 times weaker ($+0.11\ W\ m^{-2}$ versus $+0.45\ W\ m^{-2}$). The opposite signs of the forcings set off the differences and the total mean forcing looks quite comparable. The same can be said about the good agreement between the mean internal direct forcing with that determined by Chung ($-0.8\ W\ m^{-2}$ versus $-0.75\ W\ m^{-2}$). Comparing the forcing exerted by the individual aerosol compounds reveals that BC forcing estimate of Chung ($+1.43\ W\ m^{-2}$) is 13 times higher than estimated in this study, being close to the forcing computed by Hohenegger and Vidale [2005] with distribution of Tanré *et al.* [1984] ($+1.2\ W\ m^{-2}$). The BC distribution in the study of Chung was calculated on the basis of emissions of 1984, which are a factor of 2 higher than emissions applied in this

study. This alone cannot explain such high difference in the forcing estimates. Different optical parameters, particle size distributions and treatment of the relative humidity for the forcing calculations might serve as additional explanations. The forcing computed by Hohenegger and Vidale [2005] applying the distribution of Tanré *et al.* [1984] is positive, probably because of much higher contribution of BC to the total aerosol mass. The annual mean forcing computed by Hohenegger and Vidale [2005] with the GADS-aerosol distribution is 1.4 times weaker than ours ($-0.5\ W\ m^{-2}$ versus $-0.76\ W\ m^{-2}$). The European annual mean forcing computed by Bellouin *et al.* [2005] from satellite measurements ($-2.92\ W\ m^{-2}$) agrees well with the result of our sensitivity experiment ($-2.36\ W\ m^{-2}$). Again, this is only true for the average estimate. The forcing given by Bellouin *et al.* [2005] is negative all over Europe for all seasons (not shown), while forcing resulting from our sensitivity study is positive for large areas of Europe in spring and winter (Figure 3c). One of the reasons why our model simulates positive forcing, which could not be detected by satellites, might be that we miss a major addition of biomass burning aerosol (mostly OC) with a strongly nonuniform temporal emission distribution: vast quantities of biomass burning aerosol (predominantly scattering) are injected in regions and times of the year when our model would predict significant positive forcing. The forcing estimates presented here show a very large scatter due to different aerosol burdens, chemical composition, mixing assumptions and assumptions about aerosol size distribution and optical properties.

4. Spatial and Temporal Variations of the Aerosol Radiative Forcing

[25] In this section we analyze the spatial and temporal variation of the direct radiative forcing of internally mixed aerosol. Forcing efficiency (FE), defined as the ratio of the radiative forcing to the aerosol burden, is used as a measure of the variation in aerosol forcing independent of the aerosol pollution levels [Boucher and Theodore, 1995]. The forcing efficiency has a pronounced seasonal cycle with lowest values in November and December due to reduced incoming solar radiation (from $-50\ W(g\ aerosol)^{-1}$ to $+50\ W(g\ aerosol)^{-1}$ over most of Europe). In January to March, the positive FE over eastern Europe is strongest and reaches over $+200\ W(g\ aerosol)^{-1}$. From May to August, the negative FE is much stronger (below $-350\ W(g\ aerosol)^{-1}$) over higher latitudes because of longer hours of daily solar radiation. The negative FE is higher over water than over land, and positive FE is stronger over ice and snow. We want to discuss the interannual variation of the radiative forcing and the forcing efficiency exemplarily for the months February and August 2002 and 2003.

4.1. February

[26] The aerosol forcing depends on the aerosol load [see Marmer and Langmann, 2007]. The direct radiative forcing of internally mixed aerosol is enhanced over central Europe in February 2003, because of the higher aerosol load compared to February 2002 (Figure 4). The difference plot of aerosol forcing is initially difficult to interpret, because the sign of the forcing varies. That is why comparison of

Table 4. Annual Mean Direct Aerosol Forcing Over Europe, Results From This Study Compared With Other Publications

Author	Aerosol Type	Mixing State	Clear-Sky	All-Sky
This study	sulfate		-1.34	-0.76
<i>Koch et al.</i> [2007]	sulfate			-1.13
Chung ^a	inorganic ^b			-2.94
This study	BC		+0.12	+0.11
<i>Koch et al.</i> [2007]	BC			+0.45
Chung ^a	BC			+1.43
This study	OC		-0.17	-0.10
<i>Koch et al.</i> [2007]	POC			-0.15
Chung ^a	POC			-0.47
This study	sulfate, BC and OC	external	-1.39	-0.74
<i>Koch et al.</i> [2007]	sulfate, BC and POC	external		-0.83
Chung ^a	inorganic, ^b BC and OC	external		-1.98
<i>Hohenegger and Vidale</i> [2005] (based on GADS [<i>Hess et al.</i> , 1998])	sulfate, BC and OC	external		-0.5
<i>Hohenegger and Vidale</i> [2005] based on <i>Tanré et al.</i> [1984]	sulfate, BC and OC	external		+1.2
This study	sulfate, BC and OC	internal	-1.41	-0.80
Chung ^a	inorganic, ^b BC and OC	internal		-0.75
This study, sensitivity study	sulfate, BC and OC	internal	-2.36	-1.38
<i>Bellouin et al.</i> [2005]	total aerosol	satellite measured	-2.92	

^aBased on *Chung and Seinfeld* [2002] with the inorganic aerosol system simulated online following methodology of *Adams et al.* [1999, 2001] and with updated HNO_3 field from the Harvard-GISS GCM [*Mickley et al.*, 1999].

^bIncluding SO_4 , NH_4 , NO_3 .

different forcing distributions should be regarded carefully. The forcing changed signs from negative to positive over Greece and eastern Turkey between February 2002 and 2003, the areas with less aerosol burden in February 2003 than February 2002. The reason for this is that the surface albedo in February 2003 is much higher over northern, eastern and south eastern Europe and over the Alps because of snow, and in northern Baltic Sea because of the sea ice (Figure 5). The areas with enhanced surface albedo correspond to the areas of increased positive forcing (Table 5). This increase is larger for areas with higher aerosol burden.

[27] Forcing efficiency is highly variable reaching from over +200 to below $-350 \text{ W}(\text{g aerosol})^{-1}$. Changes in

surface albedo of 0.5 can cause an increase in positive FE of up to $+200 \text{ W}(\text{g aerosol})^{-1}$ over eastern Europe and the Baltic Sea, and even change its sign from -100 to $+100 \text{ W}(\text{g aerosol})^{-1}$ (Figure 5). This behavior is typical for partially absorbing aerosols [*Haywood and Shine*, 1995]. The cloud albedo has similar effect on the FE (Figure 6). The presence of clouds reduces the negative and enhances the positive FE: over water, strong negative forcing of up to $-350 \text{ W}(\text{g aerosol})^{-1}$ is reduced to $-50 \text{ W}(\text{g aerosol})^{-1}$, over western Europe and Scandinavia it changes sign from negative to positive, and over eastern Europe the positive forcing is enhanced. The contribution of the absorbing BC to the total aerosol load over these areas remains constant

REMOTE, Direct short wave forcing, internal [W/m^2]

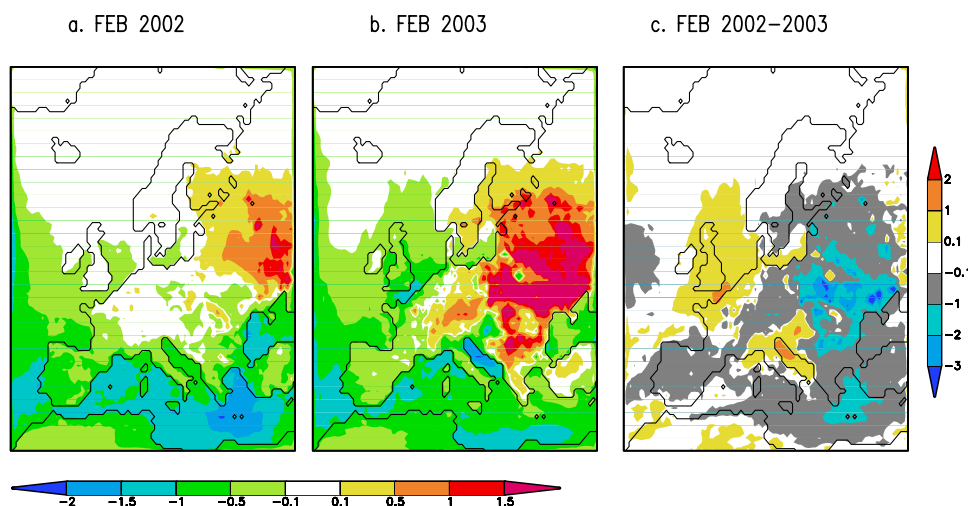


Figure 4. Monthly mean direct radiative forcing of internally mixed aerosol in (a) February 2002 and (b) February 2003 and (c) the difference plot 2002–2003 (W m^{-2}).

REMOTE, surface albedo and forcing efficiency (internal mixture)

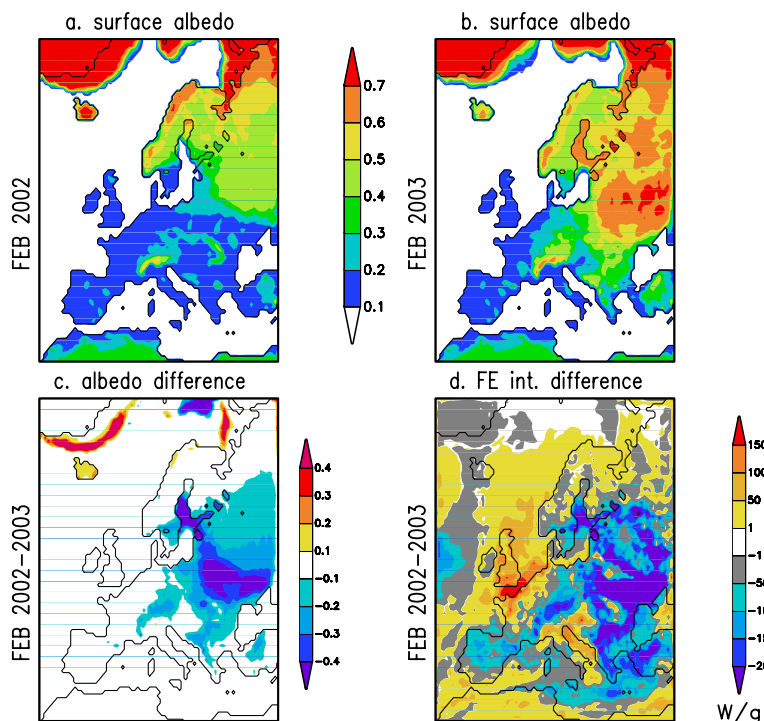


Figure 5. Monthly mean surface albedo, February (a) 2002 and (b) 2003, (c) surface albedo difference plot 2002–2003, and (d) FE difference plot 2002–2003 ($W(g\ aerosol)^{-1}$).

for both years (Table 5), we can attribute the increase of the positive FE to the surface and cloud albedo enhancement. Enhanced relative humidity causes water uptake of aerosol particles, increasing their specific extinction. We have run a sensitivity test where the influence of the relative humidity on specific extinction was turned off and have calculated the FE for this simulation (Figure 7). Both positive and negative forcing efficiencies are affected: The forcing efficiency due to the relative humidity accounts for up to $-200\ W(g\ aerosol)^{-1}$ over the Mediterranean Sea and up to $+300\ W(g\ aerosol)^{-1}$ over eastern Europe. For the negative FE, this effect is larger in February 2003 because of higher RH values over the areas with negative forcing (Table 5). The effect of RH on aerosol scattering might be overestimated in our simulations, because its effect on the asymmetry factor has not been considered in the model (section 2.2).

4.2. August

[28] The direct radiative forcing is negative in August, except for a positive forcing over Cherepovec in Russia, one of the strongest emission sources of BC (Figure 8). The positive FE over this source strongly depends on the contribution of BC to the chemical composition of the internally mixed aerosol (Table 6), which is higher in August 2003. In August 2002, the negative forcing is stronger over Scandinavia and northwestern Russia; in 2003, over the rest of Europe. The forcing efficiency regionally varies between 0 and below $-350\ W(g\ aerosol)^{-1}$.

While clouds reduce the negative FE all over Europe in August 2002, in 2003 only northern Europe is affected (Figure 9). The reduction is most significant in August 2002 over the North Atlantic and northern Russia, from below $-350\ W(g\ aerosol)^{-1}$ to $-100\ W(g\ aerosol)^{-1}$. Over central Europe, all-sky FE is 50 to $100\ W(g\ aerosol)^{-1}$ weaker than the clear-sky FE. In August 2003, clouds change the sign of the forcing from negative to positive over Cherepovec in Russia (Table 6). The effect of relative humidity over the North Atlantic and over higher latitudes is stronger in August than in February: in August, the relative humidity causes here an increase of FE of up to $-300\ W(g\ aerosol)^{-1}$ (Figure 10). Similar to cloud cover, the relative humidity is lower over central and southern Europe in August 2003 compared to 2002, but the effect is opposite: clouds reduce the negative FE, relative humidity enhances both, negative and positive FE.

[29] Because of RH and clear-sky conditions, the FE in August 2002 is 100 to $150\ W(g\ aerosol)^{-1}$ stronger over Scandinavia compared to 2003 (Figure 10c); the aerosol burden is also slightly higher [see *Marmar and Langmann, 2007*]. Together with stronger FE, this results in up to $2\ W\ m^{-2}$ stronger forcing over Scandinavia in August 2002 (Figure 8). Over the Mediterranean Sea, the FE in August 2002 is also stronger than in 2003 ($50\ \text{to}\ 100\ W(g\ aerosol)^{-1}$), mainly because of relative humidity. However, the aerosol burden over the Mediterranean Sea in August

Table 5. Mean Values for February 2002 and 2003

	Parameter	Feb 2002	Feb 2003
Emissions, SO _x	mean, Mg/mon	219.24	219.24
Anthropogenic VOC	mean, Mg/mon	171.28	171.28
POC	mean, Mg/mon	12.76	12.76
BC	mean, Mg/mon	10.15	10.15
Total aerosol load	mean, mg/m	2.59	2.93
BC contribution	pos. mean, ^a %	5	5
	neg. mean, ^b %	0	0
RH ^c	pos. mean, ^a %	85.8	70.6
	neg. mean, ^b %	76.0	74.9
Surface albedo	pos. mean, ^a	0.40	0.51
	neg. mean, ^b	0.20	0.20
Cloud cover	pos. mean, ^a	0.83	0.72
	neg. mean, ^b	0.56	0.59
FE, externally mixed	w. pos. mean, ^d W/g	+3.6	+16.4
Externally mixed	w. neg. mean, ^e W/g	-89.4	-85.4
Internally mixed	w. pos. mean, ^d W/g	+18.2	+43.4
Internally mixed	w. neg. mean, ^e W/g	-90.3	-86.1
Internal, clear-sky	w. pos. mean, ^d W/g	+10.6	+36.3
Internal, clear-sky	w. neg. mean, ^e W/g	-227.1	-241.6
Internal, no RH	w. pos. mean, ^d W/g	+2.4	+9.7
Internal, no RH	w. neg. mean, ^e W/g	-55.8	-40.0

^aAverage over areas with positive forcing (internal mixture).

^bAveraged over areas with negative internal forcing (internal mixture).

^cMean RH for the lowest 1000 m of the atmosphere, where the aerosol concentration dominates.

^dWeighted mean of the positive forcing efficiency.

^eWeighted mean of the negative forcing efficiency.

2002 is $4 \text{ mg(m}^{-2}\text{)}$ lower than in 2003, thus the forcing is 1 to 2 W m^{-2} weaker, despite the stronger FE.

5. Conclusions

[30] The variability of aerosol radiative forcing depends primarily on the tempo-spatial aerosol distribution. The mixing state of the aerosol influences strength, regional distribution and the sign of the forcing, thereby regulating the forcing efficiency. The assumptions made for the internally mixed aerosol particles lead to an enhancement of both negative and positive forcing efficiencies, compared to the external mixture. Under an assumption of externally mixed aerosols the forcing is almost everywhere negative, with the absorbing black carbon overpowered by the scattering sulfate aerosol. When mixed internally, absorption of the aerosol is enhanced, resulting in positive aerosol forcing in spring and winter over eastern and southeastern Europe. The enhancement of the negative forcing is due to the assumed size distribution. In the real world, the mixing state of aerosol is expected to affect the aerosol load through solubility, which would then have an impact on the forcing. Since in our chemistry climate model the mixing state of aerosols is not considered, this effect was not simulated.

[31] The forcing efficiency also depends on meteorological parameters: the incoming solar radiation strength and daily duration determine the regional seasonality of the forcing efficiency. Over high latitudes, FE is almost negli-

REMOTE, forcing efficiency (internal mixture)

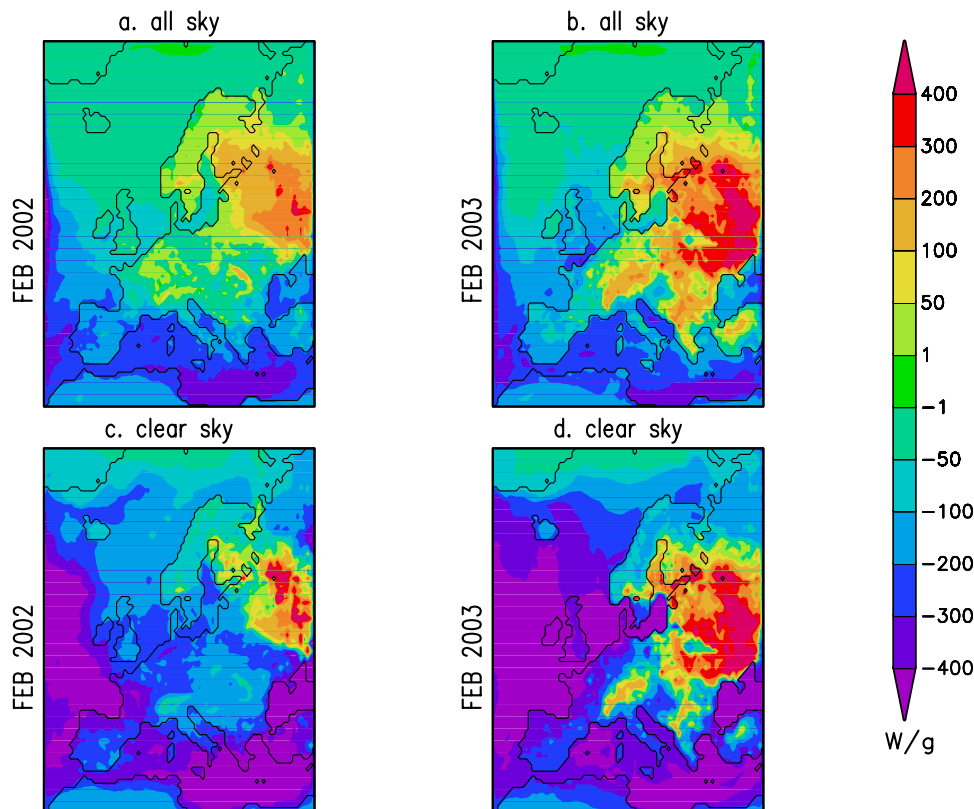


Figure 6. FE with clouds for February (a) 2002 and (b) 2003 and clear-sky for February (c) 2002 and (d) 2003 (W(g aerosol)^{-1}).

REMOTE, effect of the relative humidity on the forcing efficiency

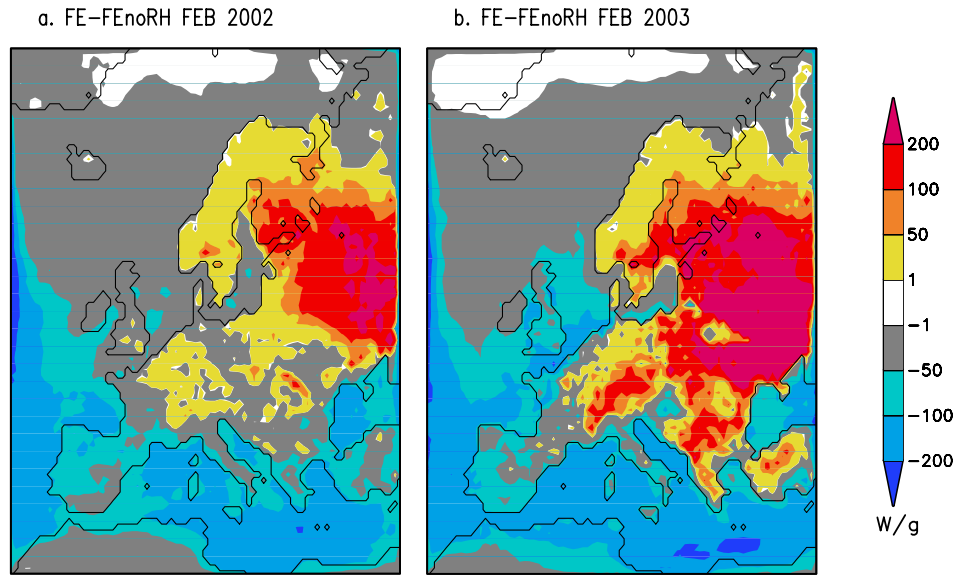


Figure 7. Difference of forcing efficiency with and without regarding relative humidity ($W(g \text{ aerosol})^{-1}$), February (a) 2002 and (b) 2003.

gible during winter and much stronger during summer. During the cold season, direct forcing is also very sensitive to the surface albedo. Enhanced surface albedo due to snow cover and sea ice can turn the sign of the forcing from negative to positive and enhance the positive forcing. This was demonstrated exemplarily for February 2002 versus 2003: increased aerosol load in 2003 resulted in enhanced positive radiative forcing, because large parts of the continent were covered by snow in contrast to the warmer winter 2002. The effect reached very high latitudes despite the limited hours of solar radiation. In March, the aerosol

burden in 2003 was even higher than in February, but this had very little effect on the forcing, because most parts of central Europe were snow free. For all seasons, relative humidity and cloud cover influenced the forcing efficiency. Clouds reduce the mean negative forcing efficiency by a factor of 1.6 (August) to 2.3 (February). Locally, the presence of clouds can change the sign of the positive forcing efficiency from negative to positive. Relative humidity can cause an increase of forcing efficiency of up to $+200 W(g \text{ aerosol})^{-1}$ and over $-200 W(g \text{ aerosol})^{-1}$.

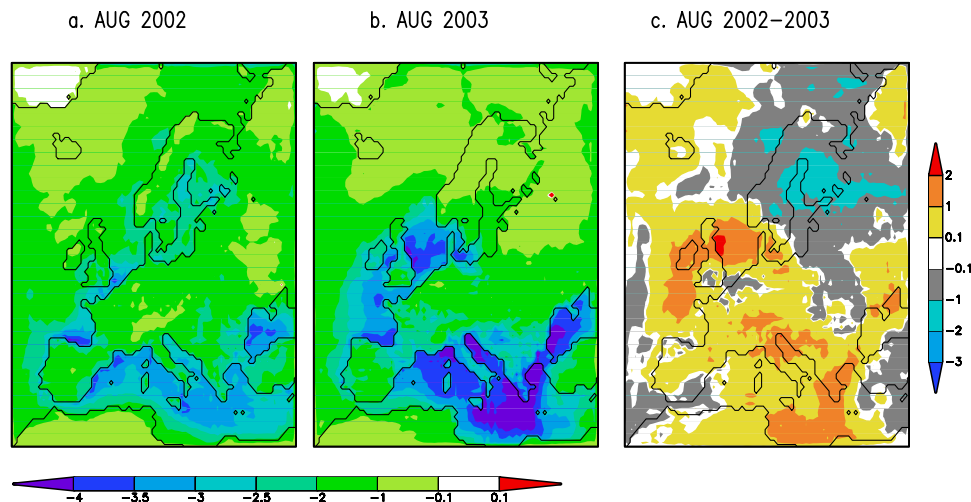
REMOTE, Direct short wave forcing, internal [W/m^2]

Figure 8. Monthly mean direct radiative forcing of internally mixed aerosol in (a) August 2002 and (b) August 2003 and (c) the difference plot 2002–2003 ($W m^{-2}$).

REMOTE, forcing efficiency (internal mixture)

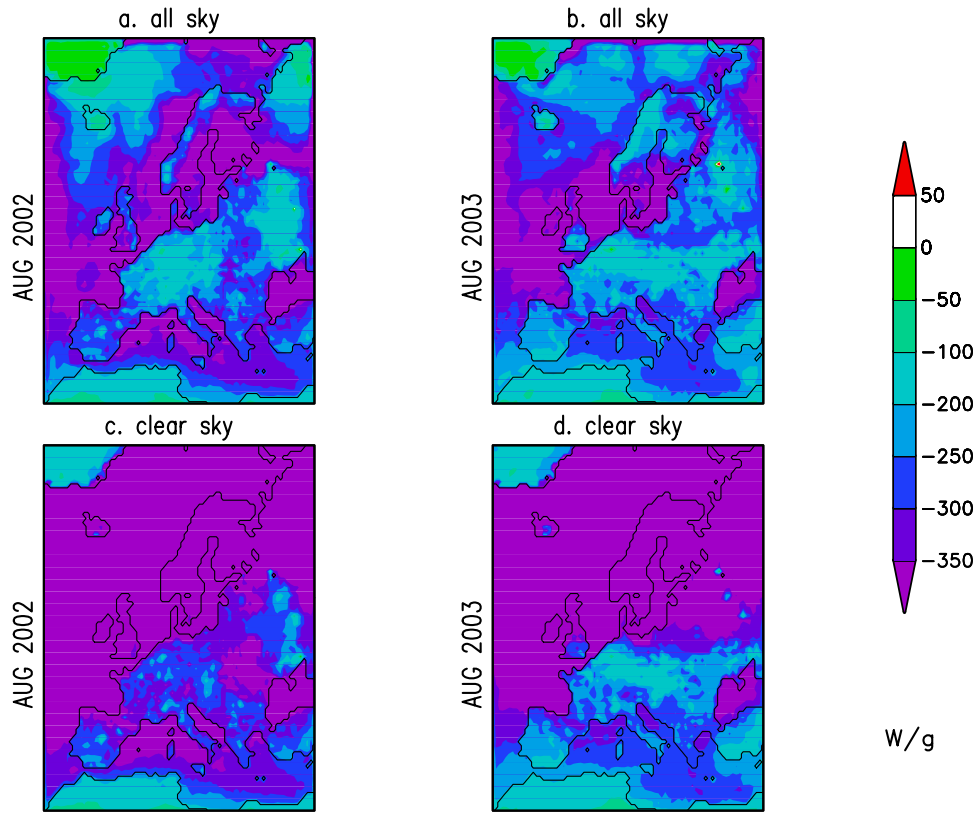


Figure 9. FE with clouds for August (a) 2002 and (b) 2003 and clear-sky for August (c) 2002 and (d) 2003 ($W(g\ aerosol)^{-1}$).

REMOTE, effect of relative humidity on the forcing efficiency

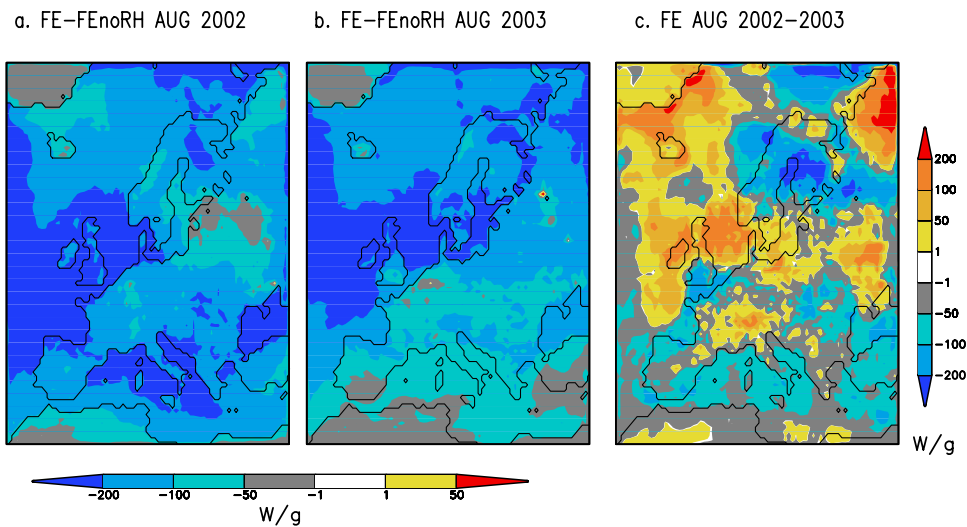


Figure 10. Difference of forcing efficiency with and without regarding relative humidity ($W(g\ aerosol)^{-1}$), August (a) 2002 and (b) 2003. (c) Difference in all-sky forcing efficiency for August, 2002–2003 ($W(g\ aerosol)^{-1}$).

Table 6. Mean Values for August 2002 and 2003

	Parameter	Aug 2002	Aug 2003
Emissions, SO _x	mean, Mg/mon	142.24	142.24
Anthropogenic VOC	mean, Mg/mon	151.71	151.71
POC	mean, Mg/mon	6.04	6.04
BC	mean, Mg/mon	6.62	6.62
Total aerosol load	mean, mg/m ²	5.31	6.34
BC contribution	pos. mean, ^a %	15	25
	neg. mean, ^b %	0	0
RH ^c	pos. mean, ^a %	54.1	71.6
	neg. mean, ^b %	68.4	63.9
Surface albedo	pos. mean ^a	0.18	0.16
	neg. mean ^b	0.14	0.14
Cloud cover	pos. mean ^a	0.27	0.49
	neg. mean ^b	0.41	0.38
FE, externally mixed	w. pos. mean, ^d W/g	–	–
Externally mixed	w. neg. mean, ^c W/g	–255.0	–240.1
Internally mixed	w. pos. mean, ^d W/g	+5.3e–03	+2.3e–02
Internally mixed	w. neg. mean, ^c W/g	–285.4	–269.2
Internal, clear-sky	w. pos. mean, ^d W/g	–	–
Internal, clear-sky	w. neg. mean, ^c W/g	–502.5	–461.3
Internal, no RH	w. pos. mean, ^d W/g	+1.0e–03	+6.8e–03
Internal, no RH	w. neg. mean, ^c W/g	–121.5	–129.9

^aAverage over areas with positive forcing (internal mixture).

^bAveraged over areas with negative internal forcing (internal mixture).

^cMean RH for the lowest 1000 m of the atmosphere, where the aerosol concentration dominates.

^dWeighted mean of the positive forcing efficiency.

^eWeighted mean of the negative forcing efficiency.

[32] In a sensitivity study we derived the direct forcing of a “realistic” aerosol burden, where we have adapted the underestimation factors from observations, 2 for black and 10 for organic carbon. We are aware of the fact that this is a coarse estimate, since the model underestimation of carbonaceous aerosol is not uniform in space and time, and the underestimation factor has only been derived from few ground based measurements. The degree of underestimation of the model compared with measurements has not been the same for all seasons. We have also applied the same factor for all vertical levels, despite the fact that the underestimation was higher for low sites than for the elevated sites, representing higher atmospheric levels [Marmier and Langmann, 2007]. Nevertheless, the result of the sensitivity study gives us a more realistic picture, than that of the base case. The radiative forcing shows very high values for summer with -2.5 to -3 W m⁻² over most parts of Europe, -3.5 W m⁻² to -4 W m⁻² over the Mediterranean and the North Sea, and a high range for winter from -2 W m⁻² over the Mediterranean Sea to $+2$ W m⁻² over the eastern Europe.

[33] **Acknowledgments.** We thank Nicolas Bellouin, Dorothy Koch, Cathy Hohenegger and Serena Chung for their forcing estimates and Melissa Pfeffer for reviewing the manuscript internally. This research was financially supported by EU project CARBOSOL.

References

- Adams, P., J. Seinfeld, and D. Koch (1999), Global concentrations of tropospheric sulfate, nitrate, and ammonium aerosol simulated in a general circulation model, *J. Geophys. Res.*, *104*, 13,791–13,824.
- Adams, P., J. Seinfeld, D. Koch, L. J. Mickley, and D. Jacob (2001), General circulation model assessment of direct radiative forcing by the sulfate-nitrate-ammonium-water inorganic aerosol system, *J. Geophys. Res.*, *106*, 1097–1112.
- Andersson-Sköld, Y., and D. Simpson (2001), Secondary organic aerosol formation in northern Europe: A model study, *J. Geophys. Res.*, *106*, 7357–7374.

- Bellouin, N., O. Boucher, J. Haywood, and M. S. Reddy (2005), Global estimate of aerosol direct radiative forcing from satellite measurements, *Nature*, *438*, 1138–1141.
- Bohren, C. F. (1986), Applicability of effective-medium theories to problems of scattering and absorption by nonhomogeneous atmospheric particles, *J. Atmos. Sci.*, *43*, 468–475.
- Boucher, O., and L. A. Theodore (1995), General circulation model assessment of the sensitivity of direct climate forcing by anthropogenic sulfate aerosols to aerosol size chemistry, *J. Geophys. Res.*, *100*, 26,117–26,134.
- Chang, J. S., R. A. Brost, I. S. A. Isaksen, S. Madronich, P. Middleton, W. R. Stockwell, and C. J. Walcek (1987), A three-dimensional Eulerian acid deposition model: Physical concepts and formulation, *J. Geophys. Res.*, *92*, 14,681–14,700.
- Chung, S. H., and J. H. Seinfeld (2002), Global distribution and climate forcing of carbonaceous aerosols, *J. Geophys. Res.*, *107*(D19), 4407, doi:10.1029/2001JD001397.
- Chylek, P., and J. Wong (1995), Effect of absorbing aerosols on global radiation budget, *J. Geophys. Res.*, *100*, 16,235–16,232.
- Cooke, W., C. Liou, H. Cachier, and J. Feichter (1999), Construction of a 1° × 1° fossil fuel emission data set for carbonaceous aerosol and implementation and radiative impact in the ECHAM4 model, *J. Geophys. Res.*, *104*(D18), 22,137–22,162.
- Fenn, R. W., S. A. Clough, W. O. Gallery, R. E. Good, F. X. Kneizys, J. D. Mill, L. S. Rothman, E. P. Shettle, and F. E. Volz (1985), Optical and infrared properties of the atmosphere, in *Handbook of Geophysics and Space Environment*, vol. 18, pp. 1–27, Air Force Geophys. Lab., Hanscom Air Force Base, Bedford, Mass.
- Gelencsér, A., B. May, D. Simpson, H. Puxbaum, D. Wagenbach, C. Pio, A. Kasper-Giebl, and M. Legrand (2007), Source apportionment of PM_{2.5} organic aerosol over Europe: Primary/secondary, natural/anthropogenic, and fossil/biogenic origin, *J. Geophys. Res.*, *112*, D23S04, doi:10.1029/2006JD008094.
- Guenther, A., R. Monson, and R. Fall (1991), Isoprene and monoterpene emission rate variability: Observations with eucalyptus and emission rate algorithm development, *J. Geophys. Res.*, *96*, 10,799–10,808.
- Guenther, A., P. Zimmermann, P. Harley, R. Monson, and R. Fall (1993), Isoprene and monoterpene emission rate variability: Model evaluations and sensitivity analyses, *J. Geophys. Res.*, *98*, 12,608–12,617.
- Hagemann, S. (2002), An improved land surface parameter dataset for global and regional climate models, *MPI Rep. 336*, Max-Planck-Inst. for Meteorol., Hamburg, Germany.
- Haywood, J., and O. Boucher (2000), Estimates of the direct and indirect radiative forcing due to tropospheric aerosols: A review, *Rev. Geophys.*, *38*, 513–543.
- Haywood, J., and K. Shine (1995), The effect of anthropogenic sulfate and soot on the clear-sky planetary radiation budget, *Geophys. Res. Lett.*, *22*(5), 603–606.
- Haywood, J. M., D. L. Robert, A. Slingo, J. M. Edwards, and K. P. Shine (1997), General circulation model calculations of the direct radiative forcing by anthropogenic sulfate and fossil-fuel soot aerosol, *J. Clim.*, *10*, 1562–1577.
- Hess, M., P. Koepke, and I. Schult (1998), Optical properties of aerosols and clouds: The software package OPAC, *Bull. Am. Meteorol. Soc.*, *79*, 831–844.
- Hitzenberger, R., and H. Puxbaum (1993), Comparisons of the measured and calculated specific absorption coefficient for Vienna urban aerosol samples, *Aerosol Sci. Technol.*, *18*, 323–345.
- Hitzenberger, R., and S. Tohno (2001), Comparison of black carbon (BC) aerosols in two urban areas (Uji, Japan and Vienna, Austria)—Concentrations and size distributions, *Atmos. Environ.*, *35*, 2089–2100.
- Hodzic, A., S. Madronich, B. Bohn, S. Massie, L. Menut, and C. Wiedinmyer (2007), Wildfire particulate matter in Europe during summer 2003: Mesoscale modeling of smoke emissions, transport and radiative effects, *Atmos. Chem. Phys. Disc.*, *7*, 4705–4760.
- Hohenegger, C., and P. Vidale (2005), Sensitivity of the European climate to aerosol forcing as simulated with a regional model, *J. Geophys. Res.*, *110*, D06201, doi:10.1029/2004JD005335.
- Horowitz, L., S. Walter, D. Mauzerall, L. Emmons, P. Rasch, C. Granier, X. Tie, J.-F. Lamarque, M. Schultz, and G. Brasseur (2003), A global simulation of tropospheric ozone and related tracers: Description and evaluation of MOZART, version 2, *J. Geophys. Res.*, *108*(D24), 4784, doi:10.1029/2002JD002853.
- Jacob, D. (2001), A note to the simulation of the annual and inter-annual variability of the water budget over the Baltic sea drainage basin, *Meteorol. Atmos. Phys.*, *77*, 61–73.
- Kanakidou, M., K. Tsigaridis, F. Dentener, and P. Crutzen (2000), Human-activity-enhanced formation of organic aerosols by biogenic hydrocarbon oxidation, *J. Geophys. Res.*, *105*, 9243–9254.
- Kanakidou, M., et al. (2005), Organic aerosol and global climate modelling: A review, *Atmos. Chem. Phys.*, *5*, 1053–1123.

- Kasper-Giebl, A., A. Koch, R. Hitznerberger, and H. Puxbaum (2000), Scavenging efficiency of “Aerosol Carbon” and sulfate in supercooled clouds at Mt. Sonnblick (3106 m a.s.l., Austria), *J. Atmos. Chem.*, *35*, 33–46.
- Koch, D., T. C. Bond, D. Streets, N. Unger, and G. R. van der Werf (2007), Global impacts of aerosols from particular source regions and sectors, *J. Geophys. Res.*, *112*, D02205, doi:10.1029/2005JD007024.
- Koepke, P., M. Hess, I. Schult, and E. Shettle (1994), Global aerosol data set, paper presented at Fourth International Aerosol Conference, Am. Assoc. for Aerosol Res., Los Angeles, Calif.
- Køltzow, M., and S. Eastwood (2002), Comparison between temperature dependent parameterization schemes for snow albedo and estimated snow albedo from AVHRR, *Res. Note 98*, Norw. Meteorol. Inst., Oslo, Norway.
- Køltzow, M., S. Eastwood, and J. E. Haugen (2003), Parameterization of snow and sea ice albedo in climate models, *Res. Rep. 149*, Norw. Meteorol. Inst., Oslo, Norway.
- Langmann, B. (2000), Numerical modelling of regional scale transport and photochemistry directly together with meteorological processes, *Atmos. Environ.*, *34*, 3585–3598.
- Langmann, B., M. Herzog, and H. F. Graf (1998), Radiative forcing of climate by sulfate aerosols as determined by a regional circulation chemistry transport model, *Atmos. Environ.*, *32*, 2757–2768.
- Lesins, G., P. Chylek, and U. Lohmann (2002), A study of internal and external mixing scenarios and its effect on aerosol optical properties and direct radiative forcing, *J. Geophys. Res.*, *107*(D10), 4094, doi:10.1029/2001JD000973.
- Mallet, M., J. C. Roger, S. Despiou, J. P. Putaud, and O. Dubovik (2004), A study of the mixing state of black carbon in urban zone, *J. Geophys. Res.*, *109*, D04202, doi:10.1029/2003JD003940.
- Marmier, E., and B. Langmann (2007), Regional aerosol modeling: 1. Inter-annual variability of aerosol distribution over Europe, *J. Geophys. Res.*, doi:10.1029/2006JD008113, in press.
- Mickley, L. J., P. P. Murti, D. J. Jacob, J. A. Logan, D. M. Koch, and D. Rind (1999), Radiative forcing from tropospheric ozone calculated with a unified chemistry-climate model, *J. Geophys. Res.*, *104*(D23), 30,153–30,172.
- Middlebrook, A., D. Murphy, and D. Thomson (1998), Observations of organic material in individual marine particles at Cape Grim during the First Aerosol Characterization Experiment (ACE 1), *J. Geophys. Res.*, *103*, 16,475–16,483.
- Murphy, D., and D. Thomson (1997), Chemical composition of single aerosol particles at Idaho Hill, *J. Geophys. Res.*, *102*, 6341–6368.
- Myhre, G., F. Stordal, K. Restad, and I. S. A. Isaksen (1998), Estimates of the direct radiative forcing due to sulfate and soot aerosols, *Tellus, Ser. B*, *50*, 463–477.
- Nemesure, S., R. Wagner, and S. E. Schwartz (1995), Direct shortwave forcing of climate by the anthropogenic sulfate aerosol: Sensitivity to particle size, composition and relative humidity, *J. Geophys. Res.*, *100*, 26,105–26,116.
- Penner, J., C. Chuang, and K. Grant (1998), Climate forcing by carbonaceous and sulfate aerosols, *Clim. Dyn.*, *14*, 836–851.
- Puxbaum, H., and M. Tenze-Kunit (2003), Size distribution and seasonal variation of atmospheric cellulose, *Atmos. Environ.*, *37*, 3693–3699.
- Roeckner, E. (1996), The atmospheric general circulation model ECHAM4: Model description and simulation of present-day climate, *MPI Rep. 218*, Max-Planck-Inst. for Meteorol., Hamburg, Germany.
- Roesch, A., M. Wild, H. Gilgen, and A. Ohmura (2001), A new snow cover fraction parametrization for the ECHAM4 GCM, *Clim. Dyn.*, *17*, 933–946.
- Schell, B. (2000), Die Behandlung sekundärer organischer Aerosole in einem komplexen Chemie-Transport-Modell, Ph.D. thesis, Univ. of Cologne, Cologne, Germany.
- Simpson, D., K. E. Yttri, Z. Klimont, K. Kupianinen, A. Caseiro, A. Gelencsér, C. Pio, H. Puxbaum, and M. Legrand (2007), Modeling carbonaceous aerosol over Europe: Analysis of the CARBOSOL and EMEP EC/OC campaigns, *J. Geophys. Res.*, *112*, D23S04, doi:10.1029/2006JD008158.
- Sloane, C. S. (1983), Optical properties of aerosols-Comparison of measurements with model calculations, *Atmos. Environ.*, *17*, 409–416.
- Sundquist, H. (1978), A parameterization scheme for non-convective condensation including prediction of cloud water content, *Q. J. R. Meteorol. Soc.*, *104*, 677–690.
- Tanré, D., J. Geleyn, and J.-M. Slingo (1984), First results of the introduction of an advanced aerosol-radiation interaction in the ECMWF low resolution global model, in *Aerosols and Their Climatic Effects: Proceeding of the Meetings of Experts*, edited by H. Gerber and A. Deepak, pp. 133-177, World Meteorol. Organ., Geneva, Switzerland.
- Tiedtke, M. (1989), A comprehensive mass flux scheme for cumulus parameterization in large scale models, *Mon. Weather Rev.*, *117*, 1779–1800.
- Toon, O. B., J. B. Pollack, and B. N. Khare (1976), The optical constants of several atmospheric aerosol species: Ammonium sulfate, aluminium oxide, and sodium chloride, *J. Geophys. Res.*, *81*(30), 5733–5748.
- Turpin, B. J., and H. Lim (2001), Species contributions to PM_{2.5} mass concentrations: Revisiting common assumption for estimating organic mass, *Aerosol. Sci. Technol.*, *35*, 602–610.
- Vestreng, V., M. Adams, and J. Goodwin (2004), Inventory review 2004. Emission data reported to CLRTAP and under the NEC directive, EMEP/EEA Joint Review Report, *Tech. Rep. EMEP-MSCW Rep. 1/2004*, Norw. Meteorol. Inst., Oslo, Norway.
- Wehrli, C. (1985), Extraterrestrial solar spectrum, *Tech. Rep. Publ. 615*, World Radiat. Cent., Davos, Switzerland.
- K. Hungershöfer, Laboratoire Interuniversitaire des Systèmes Atmosphériques, Centre National de la Recherche Scientifique/Université Paris 7 and 12, F-94010 Créteil, France. (hungershoefer@lisa.univ-paris12.fr)
- B. Langmann, Department of Experimental Physics, National University of Ireland, Galway, Ireland. (baerbel.langmann@zmaw.de)
- E. Marmier, Institute for Environment and Sustainability, European Commission-Joint Research Centre, I-21020 Ispra, Italy. (elina.marmier@jrc.it)
- T. Trautmann, Remote Sensing Technology Institute, German Aerospace Centre, D-82230 Wessling, Germany. (thomas.trautmann@dlr.de)